An updated anthropogenic CO_2 inventory in the Atlantic Ocean

K. Lee,[1] S.-D. Choi,[1] G.-H. Park,[1] R. Wanninkhof,[2] T.-H. Peng,[2] R. M. Key,[3] C. L. Sabine,[4] R. A. Feely,[4] J. L. Bullister,[4] F. J. Millero,[5] and Alex Kozyr[6]

Received 18 March 2003; revised 9 September 2003; accepted 9 October 2003; published 13 December 2003

[1] This paper presents a comprehensive analysis of the basin-wide inventory of anthropogenic CO_2 in the Atlantic Ocean based on high-quality inorganic carbon, alkalinity, chlorofluorocarbon, and nutrient data collected during the World Ocean Circulation Experiment (WOCE) Hydrographic Program, the Joint Global Ocean Flux Study (JGOFS), and the Ocean-Atmosphere Carbon Exchange Study (OACES) surveys of the Atlantic Ocean between 1990 and 1998. Anthropogenic CO_2 was separated from the large pool of dissolved inorganic carbon using an extended version of the ΔC^* method originally developed by *Gruber et al.* [1996]. The extension of the method includes the use of an optimum multiparameter analysis to determine the relative contributions from various source water types to the sample on an isopycnal surface. Total inventories of anthropogenic CO_2 in the Atlantic Ocean are highest in the subtropical regions at 20°–40°, whereas anthropogenic CO_2 penetrates the deepest in high-latitude regions (>40°N). The deeper penetration at high northern latitudes is largely due to the formation of deep water that feeds the Deep Western Boundary Current, which transports anthropogenic CO_2 into the interior. In contrast, waters south of 50°S in the Southern Ocean contain little anthropogenic CO_2. Analysis of the data collected during the 1990–1998 period yielded a total anthropogenic CO_2 inventory of 28.4 ± 4.7 Pg C in the North Atlantic (equator-70°N) and of 18.5 ± 3.9 Pg C in the South Atlantic (equator-70°S). These estimated basin-wide inventories of anthropogenic CO_2 are in good agreement with previous estimates obtained by *Gruber* [1998], after accounting for the difference in observational periods. Our calculation of the anthropogenic CO_2 inventory in the Atlantic Ocean, in conjunction with the inventories calculated previously for the Indian Ocean [*Sabine et al.*, 1999] and for the Pacific Ocean [*Sabine et al.*, 2002], yields a global anthropogenic CO_2 inventory of 112 ± 17 Pg C that has accumulated in the world oceans during the industrial era. This global oceanic uptake accounts for approximately 29% of the total CO_2 emissions from the burning of fossil fuels, land-use changes, and cement production during the past 250 years. *INDEX TERMS:* 1615 Global Change: Biogeochemical processes (4805); 1635 Global Change: Oceans (4203); 4805 Oceanography: Biological and Chemical: Biogeochemical cycles (1615); 4806 Oceanography: Biological and Chemical: Carbon cycling; *KEYWORDS:* anthropogenic CO_2, Atlantic Ocean, air-sea disequilibrium

Citation: Lee, K., et al., An updated anthropogenic CO_2 inventory in the Atlantic Ocean, *Global Biogeochem. Cycles*, *17*(4), 1116, doi:10.1029/2003GB002067, 2003.

1. Introduction

[2] The burning of fossil fuels, land-use changes, and cement production over the last 250 years have increased the atmospheric carbon dioxide (CO_2) concentration from 280 parts per million by volume (ppm) prior to the industrial revolution to the current level of more than 370 ppm [*Neftel et al.*, 1985; *Keeling and Whorf*, 2000; *Houghton et al.*, 2001]. During this period, only about half of the CO_2 released by these anthropogenic processes has remained in the atmosphere. The ocean and land biosphere are believed to have taken up the remainder [*Houghton et al.*, 2001; *Orr et al.*, 2001; *Sarmiento and Gruber*, 2002]. Of the three major sinks in the global carbon budget, that is, the atmosphere, ocean, and land biosphere, the change in

[1]School of Environmental Science and Engineering, Pohang University of Science and Technology, Pohang, Republic of Korea.
[2]Atlantic Oceanographic and Meteorological Laboratory, NOAA, Miami, Florida, USA.
[3]Atmospheric and Oceanic Sciences Program, Princeton University, Princeton, New Jersey, USA.
[4]Pacific Marine Environmental Laboratory, NOAA, Seattle, Washington, USA.
[5]Rosenstiel School of Marine and Atmospheric Studies, University of Miami, Miami, Florida, USA.
[6]Carbon Dioxide Information Analysis Center, Environmental Sciences Division, Oak Ridge National Laboratory, U.S. Deparment of Energy, Oak Ridge, Tennessee, USA.

0886-6236/03/2003GB002067$12.00

atmospheric CO_2 concentration over time has been most accurately determined, due to the presence of a high-quality global sampling network that can adequately resolve the spatial and temporal variability of atmospheric CO_2. Determination of the oceanic sink of CO_2 is a more complex task because it is difficult to sample the ocean adequately and to separate out the small anthropogenic signal from the large background concentration of the total inorganic carbon pool. The most challenging measurement problems are associated with estimating the terrestrial carbon sink because of the large spatial inhomogeneity in terrestrial carbon sources and sinks. Predicting global climate change as a consequence of CO_2 emissions requires measurements spanning long periods along with carbon models that estimate the growth rate of CO_2 in the atmosphere and its removal, redistribution, and storage in the oceans and land biosphere.

[3] During the period 1980–1989, the carbon inventory in the world oceans had increased at a mean rate of 1.9 ± 0.6 Pg C yr^{-1} (Pg C = 10^{15} g of carbon) [*Houghton et al.*, 2001], accounting for 35% of the 5.5 Pg C released annually to the atmosphere [*Houghton et al.*, 2001]. However, currently available estimates of the oceanic carbon inventory were determined based either on measurements other than CO_2 [*Quay et al.*, 1992; *Keeling and Shertz*, 1992; *Enting et al.*, 1995] or on ocean models evaluated with the bomb radiocarbon and/or CFC distribution [*Sarmiento and Sundquist*, 1992; *Siegenthaler and Sarmiento*, 1993; *Stocker et al.*, 1994; *Orr et al.*, 2001; *Dutay et al.*, 2002]. A caveat associated with these techniques is that neither bomb radiocarbon nor the more recently introduced CFCs are ideal surrogates for tracing the distribution of anthropogenic CO_2 in the oceans. The uncertainty of current estimates of oceanic uptake is ±0.6 Pg C yr^{-1} [*Houghton et al.*, 2001], which is close to the level of agreement between different models. Much of this uncertainty can be attributed to lack of direct measurements of the carbon content of the oceans at different times. In fact, the desire to reduce this uncertainty was an important factor motivating the inclusion of a global CO_2 survey as a major component of Joint Global Ocean Flux Study (JGOFS) during the 1990–1998 period. Specifically, the survey aimed to (1) quantify the uptake of anthropogenic CO_2 by the oceans, (2) improve ocean carbon cycle modeling by providing a global description of the inorganic carbonate system, and (3) characterize the transport of CO_2 in the ocean. Prior to the global CO_2 survey, these issues could only be studied on a global scale by the use of models. Many investigators participated in this global CO_2 survey. Despite the large number of the collaborating groups, however, an internally consistent basin-wide data set was obtained by the use of the state-of-art measurement techniques [*Johnson et al.*, 1993; *Millero et al.*, 1993; *Wanninkhof and Thoning*, 1993; *Clayton and Byrne*, 1993; *Neill et al.*, 1997], laboratory-calibrated measurement protocols and post-cruise adjustments. The quantity and quality of these field data are sufficient to serve as a baseline against which future measurements of the transient invasion of anthropogenic CO_2 can be compared.

[4] To quantify the anthropogenic CO_2 in the ocean, it is necessary to correct the measured concentration of total inorganic carbon (C_T) of a water sample for changes that may have occurred since the sample was isolated from the surface, for example, changes due to remineralization of organic matter or dissolution of $CaCO_3$ particles. This corrected C_T is subtracted from the "preformed C_T" of the sample, which refers to the C_T when the sample was at the outcrop region. The resulting C_T is the amount of anthropogenic CO_2 stored in the water mass. This approach was first introduced by *Brewer* [1978] and *Chen and Millero* [1979], and was subsequently applied by *Chen* [1993] to various regions of the world oceans. However, this approach has been found to suffer from significant problems, including a large uncertainty in the estimation of the preformed C_T of different water masses in the preindustrial era [*Broecker et al.*, 1985], inadequate treatment of the effect of mixing of different water types [*Shiller*, 1981], and uncertainties arising from the use of constant stoichiometric ratios and of the apparent oxygen utilization for estimating the input of CO_2 from the oxidation of organic matter [*Broecker et al.*, 1985].

[5] The shortcomings outlined above have impeded the widespread adoption of this basic approach. It was not until the mid-1990s that the basic approach was subject to further assessment and its full utility for testing anthropogenic CO_2 distributions simulated by global circulation models was realized [*Sarmiento et al.*, 1992]. Subsequent to this reassessment, *Gruber et al.* [1996] proposed an improved method, which introduces a quasi-conservative tracer ΔC^* that is the sum of the anthropogenic CO_2 concentration and the air-sea disequilibrium. This method shares the basic concept of its predecessor, but includes improved treatment of the effects of mixing of different water masses and better estimates of the values of preindustrial preformed C_T.

[6] This ΔC^* method has been applied to high-quality global CO_2 survey data collected in the Indian Ocean [*Sabine et al.*, 1999] and the Pacific Ocean [*Sabine et al.*, 2002]. Here we apply a similar ΔC^* method to inorganic carbon measurements made in Atlantic waters. The distribution of anthropogenic CO_2 in the Atlantic Ocean obtained in the present study is compared with the previous estimate [*Gruber*, 1998] made using historical data collected from the Transient Tracers in the Ocean/North Atlantic Study (TTO/NAS) and Transient Tracers in the Ocean/Tropical Atlantic Study (TTO/TAS) in 1981–1983 and from the South Atlantic Ventilation Experiment (SAVE) in 1987–1989. Our analysis, in conjunction with the analysis of *Sabine et al.* [1999] for the Indian Ocean and *Sabine et al.* [2002] for the Pacific Ocean, provides the first databased global inventory of anthropogenic CO_2 in the world oceans for the 1990s.

2. Global Survey Data Set

[7] A multinational and multiagency effort between 1990 and 1998 led to the creation of a comprehensive database of inorganic carbon measurements for the Atlantic Ocean (Figure 1, Table 1). Data used in the present study were

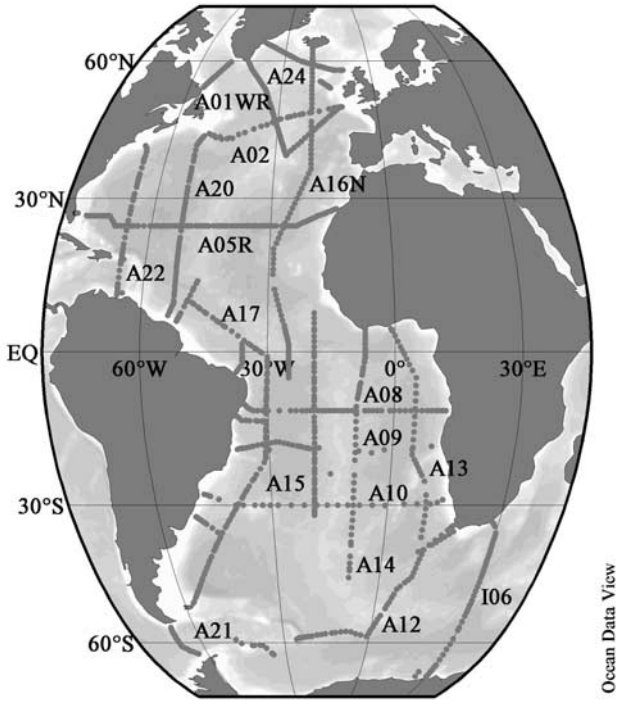

Figure 1. Locations of data used in this analysis. These data were collected between 1990 and 1998 as part of World Ocean Circulation Experiment (WOCE) Hydrographic Program, the Joint Global Ocean Flux Study (JGOFS), and the Ocean-Atmosphere Carbon Exchange Study (OACES).

collected as part of the WOCE, JGOFS, and OACES. The combined Atlantic database includes quality-controlled and cross-referenced data from a total of 23 cruises [*Wanninkhof et al.*, 2003]. Over the course of the global CO_2 survey, significant improvements were made in the measurements of C_T [*Johnson et al.*, 1993], total alkalinity (A_T) [*Millero et al.*, 1993], discrete CO_2 fugacity (fCO_2) [*Wanninkhof and Thoning*, 1993; *Neill et al.*, 1997], and pH [*Clayton and Byrne*, 1993]. Standardized methods for sampling and analysis were documented [*Dickson and Goyet*, 1994] and disseminated worldwide, which led to similar levels of accuracy and precision between investigators at sea. In particular, the use of certified reference material (CRM), developed and distributed by A. Dickson of Scripps Institution of Oceanography, contributed to improved accuracy and precision in at-sea C_T and A_T measurements [*Dickson et al.*, 2003].

[8] When measurements of A_T are not available, the combined data set also includes the calculated values of A_T from C_T and pH or C_T and fCO_2 using thermodynamic constants. The carbonic acid dissociation constants of *Merhbach et al.* [1973] as refit by *Dickson and Millero* [1987] were used in this calculation (Table 1). This set of carbonic acid dissociation constants has been shown to be the most consistent with large carbon data set collected during the global carbon survey [*Lee et al.*, 2000; *Millero et al.*, 2002]. The C_T and A_T data obtained from the 23 cruises were checked for systematic offsets of these parameters between cruises [*Wanninkhof et al.*, 2003] by four independent methods: (1) Inorganic carbon system values in deep water were compared where cruise tracks cross, referred to as ''crossover analyses''; (2) multiparameter linear regressions of C_T (or A_T) with potential temperature, salinity, oxygen, silicate, and nitrate were created for cruises which follow the same cruise track, and the

Table 1. Summary of Cruise Data Used in Calculating Anthropogenic CO_2

			Parameters Analyzed									Parameter Adjustments	
Cruise Name	Cruise Date	Chief Scientist	C_T	A_T	fCO_2	pH	CFCs	N	P	Si	O	C_T	A_T
A01WR	June 1998	P. Jones/BIO, Canada	Y[a]	Y	N[b]	N	Y	Y	Y	Y	Y	NA[c]	NA
A02	June 1997	P. Koltermann/BSH	Y	Y	N	N	Y	Y	Y	Y	Y	NA	NA
A05R	Jan. 1998	K. Lee/AOML	Y	Y + Calc[d]	Y	Y	Y	Y	Y	Y	Y	NA	NA
A08	April 1994	T. Mueller/U. of Kiel	Y	Calc[e]	Y	N	Y	Y	Y	Y	Y	NA	NA
A09	Feb. 1991	G. Siedler/KU	Y	Y	N	N	Y	Y	Y	Y	Y	NA	−7
A10	Jan. 1993	R. Onken/U. of Kiel	Y	Y	N	N	Y	Y	Y	Y	Y	NA	NA
A12	Feb. 1990	W. Roether/UB	Y	Calc[e]	Y	N	Y	Y	Y	Y	Y	NA	NA
A13	March 1995	M. Arhan/LPO	Y	Y	N	N	Y	Y	Y	Y	Y	NA	NA
A14	Jan. 1995	H. Mercier/LPO	Y	Y	N	N	Y	Y	Y	Y	Y	NA	NA
A15	April 1994	W. Smethie/LDEO	Y	Y	N	N	Y	Y	Y	Y	Y	NA	NA
A16N	July 1993	R. Wanninkhof/AOML	Y	Y	Y	Y	Y	Y	Y	Y	Y	NA	NA
A17	Feb. 1994	L. Memery/LODYC	Y	Y + Calc[d]	N	N	Y	Y	Y	Y	Y	NA	Calc[d] + 7.5
A20	July 1997	R. Pickart/WHOI	Y	Y	Y	N	Y	Y	Y	Y	Y	NA	NA
A21	Jan. 1990	W. Roether/UB	Y	Calc[f]	Y	N	Y	Y	Y	Y	Y	NA	NA
A22	Aug. 1997	T. Joyce/WHOI	Y	Y	Y	N	Y	Y	Y	Y	Y	NA	NA
A24	June 1997	L. Talley/SIO	Y	Y	N	N	Y	Y	Y	Y	Y	NA	NA
I06	March 1996	A. Poisson/France	Y	Y	N	N	Y	Y	Y	Y	Y	NA	NA

[a]Y denotes that measured values are available.
[b]N Denotes that measured values are not available.
[c]NA denotes no adjustment made.
[d]Calculated values of A_T from C_T and pH were used when measurements of A_T were not available.
[e]A_T calculated from C_T and fCO_2.
[f]A_T estimated from MLR using hydrographic parameters from nearby stations with measured A_T.

calculated values were then compared with the measured parameters for individual cruises; (3) the internal consistency between parameters was determined using thermodynamic models when more than two carbon system parameters were measured; and (4) regional multiparameter linear regressions of C_T (or A_T) with potential temperature, salinity, oxygen, silicate, and phosphate were created using data that were deemed good based on the previous checks. The calculated values were then compared with individual cruises that showed significant offsets in the crossover analysis.

[9] The results of the four analyses suggest that the inter-cruise differences for C_T and A_T are <4 and <6 μmol kg^{-1}, respectively, except for a few cruises [*Wanninkhof et al.*, 2003]. An adjustment of −7 μmol kg^{-1} was recommended for A_T values on A09, whereas no adjustments for C_T were suggested. After adjusting the A09 A_T data, the entire data set is internally consistent to ±4 for C_T and ±6 μmol kg^{-1} for A_T. The final data set comprises approximately 26,538 measurements of C_T and 20,058 measurements of A_T, and is available at http://cdiac.ornl.gov/oceans/datameta.html. The caveats in the analysis and recommendations should be borne in mind. The analysis focused primarily on deep-water quantities, and assumed that they are invariant on decadal timescales. Moreover, no comparisons were made in the upper water column, because there is seasonal variability in the upper water and the anthropogenic perturbations are most noticeable there. On the WOCE/JGOFS/OACES cruises, efforts were made to collect CFC samples from the same bottles as were used for the C_T and A_T determinations. A number of laboratories made CFC measurements as part of these programs. After the initial shipboard analysis, a variety of tests were performed to evaluate the quality of CFC data sets, including comparisons of air measurements with global atmospheric CFC trends and with measurements of surface CFC concentration, and examination of the consistency of the CFC concentration and CFC-11/CFC-12 ratio measurements along vertical profiles, along sections, and at crossover stations. The CFC data were combined with the global WOCE data set [*WOCE Data Products Committee*, 2002] and are reported as picomole per kilogram seawater (pmol kg^{-1}) on the SIO98 calibration scale. These data are available at http://cdiac.ornl.gov/oceans/datameta.html.

3. Calculation of Anthropogenic CO_2

3.1. ΔC* Calculation

[10] The amount of total inorganic carbon in the oceans is controlled by the production and remineralization of organic matter and calcium carbonate, and air-sea exchange of anthropogenic CO_2. The technique for accounting for these contributions and separating the anthropogenic CO_2 component (typically <60 μmol kg^{-1}) from the large pool of total inorganic carbon (typically 1800–2200 μmol kg^{-1}) was developed by *Gruber et al.* [1996] and refined by *Sabine et al.* [2002]. This method is based on the same general concepts as its predecessors [*Brewer*, 1978; *Chen and Millero*, 1979] but partially addresses some shortcomings inherent in the earlier methods. Specifically, this new method introduces a quasi-conservative tracer, ΔC*, defined as

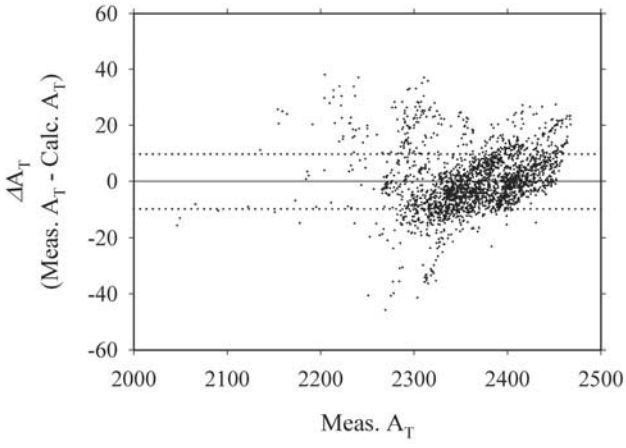

Figure 2. Residual plot of the difference between measured surface alkalinity and that estimated by multilinear regression (equation (2)) using S and NO with the measured alkalinity (pressure <100 dbar). Estimated alkalinity is based on multilinear regression using S and NO ($O_2 - R_{O:N} \times N$). The dotted line is the standard deviation from the mean (1σ = 10.3 μmol kg^{-1}).

$$\begin{aligned}\Delta C^* = {} & C_T^{MEAS} + R_{C:O}\left(O_2^{EQ} - O_2^{MEAS}\right) \\ & - 0.5\left[\left(A_T^{MEAS} - A_T^{o}\right) - R_{N:O}\left(O_2^{EQ} - O_2^{MEAS}\right)\right] \\ & - C_T^{EQ}\left(fCO_2 = 280\mu atm, A_T^{o}, \theta, S\right), \end{aligned} \quad (1)$$

where the superscript "MEAS" refers to the measured concentrations in water samples; O_2^{EQ} and O_2^{MEAS} are the saturation and in situ concentrations of oxygen, respectively; A_T^o is the preformed A_T, which is the A_T that a water parcel had when it was last at the ocean surface; C_T^{EQ} is the C_T in equilibrium with the preindustrial atmospheric CO_2 fugacity of 280 μatm for the sample's salinity (S), potential temperature (θ), and A_T^o; and $R_{C:O}$ and $R_{N:O}$ are stoichiometric ratios relating inorganic carbon and nitrate (N) changes to dissolved oxygen (O) changes, respectively.

[11] The preformed alkalinity (A_T^o) of a subsurface water parcel was estimated from a multilinear regression using conservative tracers such as S and NO as independent variables. NO is defined as $NO = O_2 - R_{O:N} \times N$ [*Broecker*, 1974]. We used $R_{O:N}$ of −10.625 taken from *Anderson and Sarmiento* [1994]. The measured surface A_T data (<100 dbars) from the WOCE/JGOFS/OACES global CO_2 survey program gave the following relationship (Figure 2):

$$A_T^o\left(\mu mol\ kg^{-1}\right) = 335.7 + 55.80 \times S + 0.08924 \times NO, \quad (2)$$

where S is on the practical salinity scale and NO is in μmol kg^{-1}. The standard error (1σ) of the estimated A_T^o is

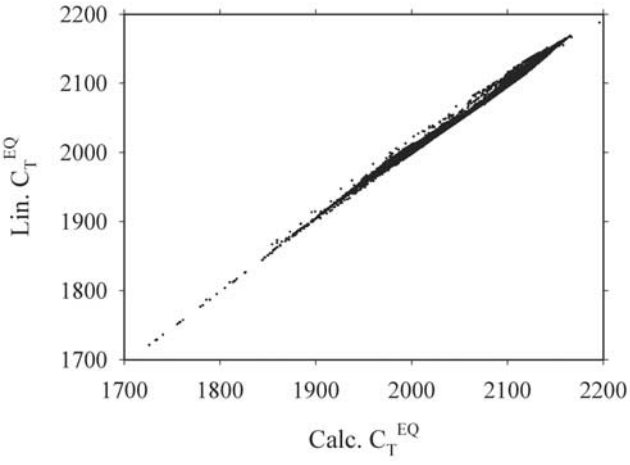

Figure 3. Plot of linearized equilibrium concentration of C_T (C_T^{EQ}) versus directly calculated C_T^{EQ} from a thermodynamic model using A_T^o from equation (2) and fCO_2 = 280 μatm.

±10.3 μmol kg^{-1} based on 2345 data points. In contrast to *Gruber et al.* [1996], who used PO ($O_2 - R_{O:P} \times P$), we used NO because gaps exist in the phosphorous data set in a zonal section of A05R and the loss of nitrate due to water column denitrification is insignificant in the Atlantic Ocean [*Gruber and Sarmiento*, 1997]. This relationship holds for the surface ocean as covered by the cruise tracks occupied during the Atlantic CO_2 survey (Figure 1). The use of an additional variable such as θ to fit surface A_T data does not reduce the uncertainty. The values of A_T^o calculated using equation (2) are on average about 5 μmol kg^{-1} higher than the corresponding values calculated using Gruber et al.'s equation derived from the GEOSECS, TTO/NAS, TTO/TAS, and SAVE surface data. This systematic offset, however, largely cancels out in the calculation of the concentration of anthropogenic CO_2 (C^{ANT}) because it equally affects ΔC* and ΔC^{DISEQ}, the difference of which is C^{ANT},

$$C^{ANT} = \Delta C^* - \Delta C^{DISEQ}. \quad (3)$$

The equilibrium value of C_T (C_T^{EQ}) with respect to a preindustrial atmospheric fugacity of 280 μatm was calculated from the estimated A_T^o from equation (2) and fCO_2 = 280 μatm using the dissociation constants for carbonic acid of *Merhbach et al.* [1973] and other ancillary constants as recommended by *Millero* [1995] and *Lee et al.* [2000]. The resulting C_T^{EQ} were then linearized by a least squares linear fit, yielding the equation

$$C_T^{EQ} = 2077 - 8.517(\theta - 9) + 3.523(S - 35) + 0.6399\left(A_T^o - 2320\right), \quad (4)$$

with a standard error (1σ) between the linearized C_T^{EQ} and calculated C_T^{EQ} of ±3.0 μmol kg^{-1} (Figure 3).

[12] The sum of the first three terms on the right side of equation (1) is the preformed C_T of a sample when the sample is at the surface. ΔC* is the difference between the preformed C_T and the C_T in equilibrium with a preindustrial atmospheric fCO_2 of 280 μatm at the values of θ, S, and A_T^o of the sample. Under these conditions, if the ocean takes in anthropogenic CO_2, the value of ΔC* will increase. Thus ΔC* reflects C^{ANT} and ΔC^{DISEQ}, expressed in terms of C_T at the time when the sample lost contact with the atmosphere. C^{ANT} can only be estimated by calculating the air-sea disequilibrium of a water parcel at the time of water mass formation at an outcrop region.

3.2. Estimation of the Air-Sea Disequilibrium

[13] For any given water parcel in the interior of the ocean, the net air-sea disequilibrium value ($\Delta C^{DISEQ\text{-}NET}$) represents a mixture of the disequilibria of the *n* different end-members,

$$\Delta C^{DISEQ-NET} = \sum_{i=1}^{n} x_i \Delta C^{DISEQ-i}, \quad (5)$$

where x_i ($\sum x_i = 1$) is the relative contribution of the particular source water type to each sample and $\Delta C^{DISEQ\text{-}i}$ is the unique disequilibrium value for the particular type of source water. This analysis is based on the assumption that anthropogenic CO_2 is predominantly transported along isopycnal surfaces and that the disequilibrium value for an outcrop region of a particular isopycnal surface has remained approximately constant over time.

[14] Determination of the air-sea CO_2 disequilibrium term (ΔC^{DISEQ}) needed for estimating C^{ANT} is not straightforward [*Gruber et al.*, 1996; *Sabine et al.*, 2002]. Two methods can be used to estimate ΔC^{DISEQ} for isopycnal layers. For isopycnal surfaces located in the interior of the ocean where CFC-12 is absent and where one can confidently assume that there is no anthropogenic CO_2 ($C^{ANT} = 0$), the ΔC^{DISEQ} term equals ΔC* ($\Delta C^{DISEQ} = \Delta C^* - [C^{ANT} = 0]$) (Table 2). The ΔC* values in these waters reflect a mixture of different end-members ΔC^{DISEQ}. To ensure that the ΔC^{DISEQ} values for deep density surfaces were not contaminated with anthropogenic CO_2, we only used ΔC* values showing no obvious trend along the isopycnal surface. However, despite these measures, we cannot completely rule out the possibility that the deep density surfaces we consider may be contaminated with anthropogenic CO_2, albeit to a minor extent. If this is the case, the ΔC* method will underestimate the amount of anthropogenic CO_2.

[15] For shallow or ventilated isopycnal surfaces that contain measurable levels of CFC-12, the assumption that the waters removed from the outcrop are devoid of anthropogenic CO_2 does not hold. For such surfaces, we used the ΔC^*_{TIME} method, which calculates the concentration of total inorganic carbon ($C_T^{EQ}{}_T$) in equilibrium with the corresponding atmospheric fCO_2 ($fCO_2^{Tsample\text{-}CFC}$) with which the water parcel was in contact during its formation (sampling date, Tsample−CFC age,

Table 2. Definitions of Water Types for the Atlantic Ocean

Water Type[a]	Latitude	Theta	SD (Theta)	S	SD (S)	O	SD (O)	PO_4	SD (PO_4)	NO_3	SD (NO_3)	Si	SD (Si)	ΔC^{DISEQ}	SD (ΔC^{DISEQ})	Method
SACW (1a)	30°S	12.51	1.13	35.12	0.15	211.50	13.00	0.83	0.18	11.08	2.89	4.39	1.42	−17.12	3.82	ΔC^*_{TIME}
NACW (1b)	50°N	10.60	0.84	35.46	0.12	241.13	13.37	0.75	0.15	11.58	1.72	4.50	1.02	−10.71	3.74	ΔC^*_{TIME}
AAIW (1c)	36°S	3.83	0.73	34.29	0.05	229.59	14.24	2.08	0.12	30.31	1.70	28.43	8.00	−17.07	3.52	ΔC^*_{TIME}
CW (1d)	23°N	21.77	1.37	37.03	0.14	198.83	11.22	0.04	0.04	0.81	0.84	0.59	0.27	−13.37	4.22	ΔC^*_{TIME}
MW (2a)	41°N	9.33	0.59	35.72	0.08	187.45	6.23	1.15	0.11	17.31	0.52	9.42	0.85	−16.67	2.44	ΔC^*_{TIME}
NACW (2b)	39°N	6.61	0.21	35.09	0.03	196.17	12.04	1.38	0.13	21.08	1.78	13.40	2.12	−23.28	1.91	ΔC^*_{TIME}
NADW (2c)	44°N	2.30	0.38	34.92	0.03	263.62	14.99	1.24	0.15	18.52	2.31	26.64	11.41	−16.90	2.87	ΔC^*
AAIW (2d)	32°S	2.85	0.18	34.55	0.03	187.96	3.38	2.24	0.06	32.69	0.83	54.45	3.91	−6.37	2.46	ΔC^*
AABW (2e)	56°S	−0.03	0.43	34.67	0.02	224.82	12.93	2.30	0.03	33.28	0.51	124.99	6.63	−7.77	4.18	ΔC^*

[a]SACW: South Atlantic Central Water; NACW: North Atlantic Central Water; AAIW: Antarctic Intermediate Water; CW: we arbitrarily named Central Water which is a mixture of SACW + NACW; MW: Mediterranean Water; NADW: North Atlantic Deep Water; and AABW: Antarctic Bottom Water.

CFC). Replacing C_T^{EQ} in equation (1) with $C_T^{EQ}{}_T$ yields ΔC^*_{TIME} in the following manner:

$$\Delta C^*_{TIME} = C_T^{MEAS} + R_{C:O}\left(O_2^{EQ} - O_2^{MEAS}\right) - 0.5\left[\left(A_T^{MEAS} - A_T^{o}\right) - R_{N:O}\left(O_2^{EQ} - O_2^{MEAS}\right)\right] - C_T^{EQ}{}_T\left(fCO_2^{Tsample-CFC}, A_T^{o}, \theta, S\right) \quad (6)$$

The age of the water parcel was calculated by converting the CFC-12 concentration (pmol kg^{-1}) in the subsurface water to the partial pressure of CFC-12 (*p*CFC-12) at the potential temperature and salinity [*Doney and Bullister*, 1992] and then matching the *p*CFC-12 of the subsurface water with the *p*CFC-12 of the atmosphere for the appropriate year. In this calculation, the subsurface water parcel is assumed to have been in solubility equilibrium when it was in contact with the overlying atmospheric *p*CFC-12. Thus the age of the subsurface water is defined as the time difference between the measurement date and the date when the water parcel was last in contact with the atmosphere. For waters with pressures <100 dbars, ΔC^{DISEQ} was determined from equation (6) under the assumption that the year in which the cruise was conducted is a good approximation for the age of waters.

[16] The water age calculated based on *p*CFC-12 will not necessarily be identical to the true water age because of possible initial undersaturation of CFC-12 in an outcrop region and systematic biases in CFC-based ages due to subsurface dilution and nonlinear mixing of waters with differing ages [*Warner et al.*, 1996; *Doney et al.*, 1997; *Sonnerup*, 2001]. For the period 1965–1990, the CFC-12 concentration in the atmosphere increased relatively rapidly [*Walker et al.*, 2000], so a CFC-12 undersaturation of 5–10% in an outcrop region would increase the initial *p*CFC-12 age by a few years relative to the true age. Age biasing can be significant when younger and older waters mix, with the *p*CFC-12-based age of the mixture tending toward the age of the younger (higher CFC-bearing) component. However, mixing between waters ventilated between 1965–1990 is expected to give rise to relatively small age biases because of the quasi-linear increase in atmospheric CFC-12 during this period [*Doney et al.*, 1997; *Sonnerup*, 2001]. In the present study we limited the use of *p*CFC-12-based ages for waters younger than 30 years old, because the difference between the true and the *p*CFC-12 age for these waters is less than 25% [*Doney et al.*, 1997; *Sonnerup*, 2001].

[17] The value of ΔC^{DISEQ} estimated for a particular water parcel represents the weighted average of individual air-sea disequilibria for various source water types. In previous studies, the net ΔC^{DISEQ} value for a certain water parcel was estimated based on the assumption of either no mixing [*Chen and Millero*, 1979] or simple two end-member mixing [*Gruber et al.*, 1996; *Gruber*, 1998] along isopycnal surfaces. Optimum multiparameter (OMP) analysis was recently adopted to improve the determination of the net air-sea disequilibrium for a sample by more accurately estimating the relative contributions of the various source waters contained in the sample [*Sabine et al.*, 2002]. Below we briefly describe the key aspects of the OMP procedure

Table 3. Weights Assigned to Linear Equations (Equations (7)–(9)) Used in the Optimum Multiparameter (OMP) Analysis

	Temperature Equation (7)	Salinity Equation (7)	Phosphate Equation (8)	Oxygen Equation (8)	Nitrate Equation (8)	Silicate Equation (8)	Mass Conservation Equation (9)
Block 1	29	56	23	2	18	3	100
Block 2	40	35	13	5	11	17	100

for estimating mixing coefficients; further details on this procedure can be found elsewhere [*Tomczak*, 1981; *You and Tomczak*, 1993; *Poole and Tomczak*, 1999].

[18] The utility of the OMP analysis lies in its ability to determine mixing coefficients from predefined source water types that are represented by unique values of measured conservative (temperature T, salinity S) and nonconservative (oxygen O, silicate Si, nitrate N, and phosphate P) parameters. The number of source water types depends on the availability of measured values for the various parameters. The OMP analysis used in the present study is the extended version that, unlike the original version, accounts for changes in source water types due to biological processes. The extended OMP analysis includes biogeochemical changes in source water types, making it suitable for investigating water mass structures on basin-wide scales. The relative contributions of source water types to each data point are estimated by minimizing the residuals (R_C or R_{NC}) of the following linear equations in the least squares sense:

$$x_1C_1 + x_2C_2 + x_3C_3 + x_4C_4 + x_5C_5 - C_{MEAS} = R_C, \quad (7)$$

$$x_1NC_1 + x_2NC_2 + x_3NC_3 + x_4NC_4 + x_5NC_5 + R_{N/P}\Delta P - NC_{MEAS} = R_{NC}, \quad (8)$$

$$x_1 + x_2 + x_3 + x_4 + x_5 = 1 + R_\Sigma, \quad (9)$$

where x_i (i = 1–5) is the relative contribution of source water type i, C_i is the conservative parameter (T, S) concentration of the source water type i, and NC_i is the nonconservative (O, Si, N, P) parameter concentration of the source water type i, the subscript "MEAS" denotes measured parameters, and equation (9) represents the condition of mass conservation ($\sum x_i$ = 1), which is an additional constraint.

[19] In the equation for the nonconservative parameters (equation (8)), the estimated change in phosphate (ΔP) due to remineralization of organic matter is related to the change in other bioactive parameters through the stoichiometric ratios (R) of *Anderson and Sarmiento* [1994], which takes care of the effect of changes in source water type definitions (see Table 2) due to biological influences. Equations (7)–(9) were normalized to make their units comparable and weighted differently to account for differences in analytical accuracy and the dynamic range of parameters in the ocean in terms of time and space. The mass conservation equation (equation (9)) is generally assigned the highest weight because the sum of the mixing coefficients should be unity. In our analysis, we initially assigned equation (9) a weight comparable to the highest of the other parameter weights and then increased this weight until the residuals were smaller than 1% (Table 3). The next highest weight was assigned to equation (7) because salinity and temperature are conservative properties. We refer readers elsewhere [*Tomczak*, 1981; *You and Tomczak*, 1993; *Poole and Tomczak*, 1999] for further details on the normalization and weighting scheme.

[20] A key step in the OMP analysis is the identification and definition of the source water types for the mixing model. The entire Atlantic data set was divided into two blocks of data according to potential density (σ_θ) (Figure 4). The first set of data was obtained from the main thermocline ($24 < \sigma_\theta < 27.5$), where there is measurable CFC-12. For this block of data, consideration of a temperature-salinity

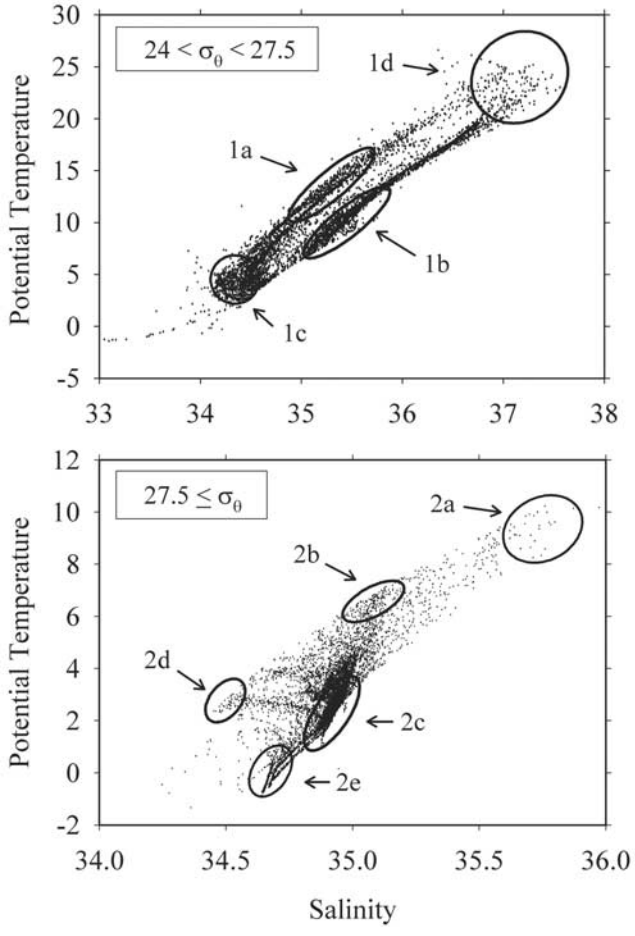

Figure 4. Temperature-salinity diagrams for all Atlantic data points on which anthropogenic CO_2 can be estimated. Data within the ovals were used for defining properties of source water types (results are summarized in Table 2).

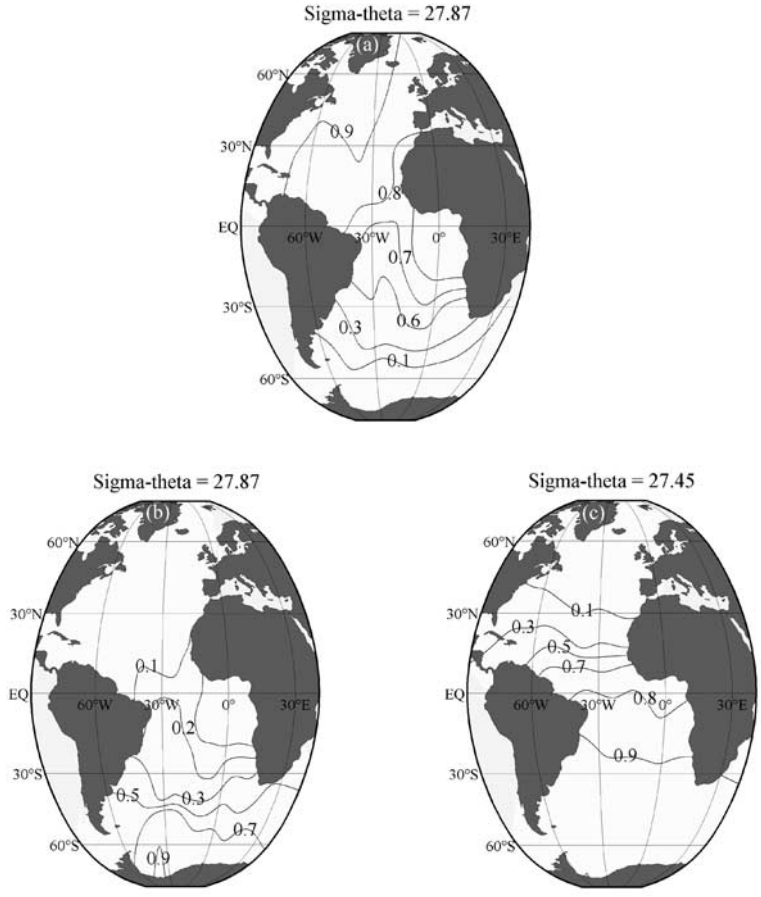

Figure 5. Maps of the OMP analysis solution, showing (a) contributions of the North Atlantic Deep Water, (b) the Antarctic Bottom Water, and (c) the Antarctic Intermediate Water.

diagram, location (latitude and depth), and descriptions of water types in the literature [*Schmitz*, 1996] revealed four source water types: South Atlantic Central Water (SACW), North Atlantic Central Water (NACW), Antarctic Intermediate Water (AAIW), and Central Water (CW, a mixture of SACW + NACW). The properties of these source waters were then determined by taking the mean and standard deviation of hydrographic data representing these source water types (see Table 2). The second data set was obtained from intermediate and deep waters ($\sigma_\theta \geq 27.5$). Five source water types were also identified in this block of data: NACW, AAIW, Mediterranean Water (MW), North Atlantic Deep Water (NADW), and Antarctic Bottom Water (AABW). The properties of these source water types were then determined using the method that was used for the main thermocline (Table 2). The distributions of the fractions of three major water types derived from the OMP analysis, shown in Figure 5, are in good agreement with the deep-water structures of the Atlantic Ocean. In addition, the definitions of source water types identified from two layers agree well with those reported by *Schmitz* [1996]. For comparison, *Gruber* [1998] estimated the relative contributions of three end-member waters using a two-end-member mixing model and the conservative tracer PO_4^*, defined as $O_2 - R_{O:P} \times P$.

[21] The net air-sea disequilibrium value ($\Delta C^{DISEQ\text{-}NET}$) for each data point in this analysis was calculated by using equation (5) along with mixing fractions for each sample (x_i) derived from the OMP analysis and the unique disequilibrium values for different source water types ($\Delta C^{DISEQ\text{-}i}$) (Table 2).

3.3. Evaluation of Errors

[22] A rigorous analysis of the error associated with the estimated values of C^{ANT} is difficult because of the subjective nature of the choices of end-member water types, preformed values, and constant remineralization coefficients. The error will consist of random and systematic components. Random errors are introduced by uncertainties in preformed A_T^o, linearized C_T^{EQ}, carbon and tracer measurements, the stoichiometric ratios ($R_{C:O}$ and $R_{N:O}$), and in the potential disequilibrium of oxygen between the surface ocean and the overlying atmosphere. These random errors can be calculated by propagating through the precision of the various measurements required in solving equation (1), as described in detail

Table 4. Mean Values of Air-Sea Disequilibrium on Density Intervals in the Atlantic Ocean Calculated by *Gruber* [1998] and Used in This Present Study[a]

	Gruber			This Study			Gruber			This Study			Gruber			This Study		
Potential Density	ΔC^{NA}, μmol kg^{-1}	σ	N	ΔC^{NA}, μmol kg^{-1}	σ	N	ΔC^{SA}, μmol kg^{-1}	σ	N	ΔC^{SA}, μmol kg^{-1}	σ	N	ΔC^{TA}, μmol kg^{-1}	σ	N	ΔC^{TA}, μmol kg^{-1}	σ	N
								σ_0 *Surfaces*										
25.30	−19	5	5	−18	6	15	4	7	15	10	6	10	13	1	2			
25.60	−17	5	2	−17	5	9	−5	5	22				17	2	3	−15	6	24
25.90	−13	8	6	−13	5	40	−12	6	23				9	4	4	−18	5	63
26.20	−24	4	7	−20	5	68	−17	2	9	−3	5	11	4	4	14	−14	5	7
26.50	−22	5	52	−21	6	410	−15	5	25	−12	5	110	−2	3	79	−15	4	93
26.80	−12	3	34	−17	5	85	−10	3	209	−14	4	313	−5	3	25	−14	5	113
27.10	−12	3	53	−14	5	549	−13	3	303	−18	3	171	−7	3	20	−16	5	130
27.30	−14	4	20	−15	6	106	−18	3	46	−20	4	86						
27.40	−17	4	13	−16	6	202	−20	4	30									
								σ_2 *Surfaces*										
36.45	−16	5	39	−16	5	265	−17	3	34									
36.55	−15	5	34	−19	5	11	−20	2	26	*								
36.65	−16	6	39	−21	4	275	−19	5	15	−23	0	57						
36.75	−18	5	60	−22	3	122	−20	3	9	−17	5	105						
36.85	−13	8	102	−15	8	823	−17	7	47	−14	4	146						
36.95	−10	4	106	−19	8	98	−17	5	48	−14	6	214						
37.00	−13	4	92	−15	5	56	−14	4	108	−16	4	51						
37.05	−16	3	94	−18	4	721	−16	3	110	−14	5	366						
								σ_4 *Surfaces*										
45.825	−16	3	51	*			−16	3	62	−14	5	44						
45.850	−16	4	49	−18	5	261	−16	4	60	−11	4	159						
45.875	−15	4	68	−18	4	317	−16	4	75	−11	5	149						
45.900	−16	3	39	−21	6	89	−16	3	45	−10	4	268						
45.925	−15	3	28	−25	2	20	−15	3	31	−10	4	127						
45.950	−15	3	15				−15	3	20	−10	4	244						
45.975							−14	3	27	−9	4	104						
46.000							−13	3	36	−9	4	284						
46.025							−12	3	30	−9	4	198						
46.050							−12	4	37	−9	3	292						

[a]Disequilibrium values are not reported when the total number of data is fewer than five.

by other investigators [*Gruber et al.*, 1996; *Sabine et al.*, 1999],

$$\left\{\sigma C^{ANT}\right\}^2 = \left\{\sigma C_T^{MEAS}\right\}^2 + \left\{\sigma C_T^{EQ}\right\}^2 + \left\{\left(O_2^{EQ} - O_2^{MEAS}\right)\sigma R_{C:O}\right\}^2 + \left\{(R_{C:O} + 0.5R_{N:O})\sigma O_2^{EQ}\right\}^2 + \left\{(-R_{C:O} - 0.5R_{N:O})\sigma O_2^{MEAS}\right\}^2 + \left\{0.5\sigma A_T^{MEAS}\right\}^2 + \left\{\left(\partial C_T^{EQ}/\partial A_T^{MEAS} + 0.5\right)\sigma A_T^{o}\right\}^2 - \left\{\sigma \Delta C^{DISEQ}\right\}^2, \quad (10)$$

where σC_T^{MEAS} = 2.0 μmol kg^{-1}; σC_T^{EQ} = 3.0 μmol kg^{-1}; σO_2^{EQ} = 4.0 μmol kg^{-1}; σO_2^{MEAS} = 1.0 μmol kg^{-1}; σA_T^{MEAS} = 4.0 μmol kg^{-1}; σA_T^{o} = 10.3 μmol kg^{-1}; $\partial C_T^{EQ}/\partial A_T^{MEAS}$ = 0.842; $\sigma \Delta C^{DISEQ}$ = 3.3 μmol kg^{-1}; $\sigma R_{C:O}$ = 0.092 μmol kg^{-1}; and $\sigma R_{N:O}$ = 0.0081 μmol kg^{-1}.

[23] The uncertainties (1σ) in the measured parameters used in equation (10) were taken from *Wanninkhof et al.* [2003] and *Gruber et al.* [1996], and those for the preformed parameters were taken from section 3.1. The uncertainty in $\sigma \Delta C^{DISEQ}$ was taken as the average value for the standard deviations (1σ) of the means for all the source water types used in the OMP analysis (see Table 2). For stoichiometric ratios, the uncertainties estimated by *Anderson and Sarmiento* [1994] were used. The error in C^{ANT} due to uncertainties in $R_{C:O}$ becomes significant only for an apparent oxygen utilization ($AOU = O_2^{EQ} - O_2^{MEAS}$) greater than 80 μmol kg^{-1} [*Gruber et al.*, 1996]. We used an AOU value of 50 μmol kg^{-1} for estimating the error in σC^{ANT} because most of the anthropogenic CO_2 is found in upper waters with AOU values of <50 μmol kg^{-1}. The overall uncertainty of our C^{ANT} estimation is 7.9 μmol kg^{-1} (equal to the error for an AOU of 50 μmol kg^{-1}), which is close to the previous estimates of 6 μmol kg^{-1} [*Sabine et al.*, 1999] and 9 μmol kg^{-1} [*Gruber et al.*, 1996]. Implicit in our error estimation is the assumption that the individual errors are unrelated and independent. Some of the errors may cause systematic biases in the C^{ANT} estimation. In particular, the uncertainties in the stoichiometric ratios, $R_{C:O}$, could potentially result in an average error of about 4 μmol kg^{-1} [*Sabine et al.*, 1999, 2002]. However, systematic errors such as those due to uncertainties in $R_{C:O}$ are partially canceled out in the present method for estimating C^{ANT} because C^{ANT} is calculated as the difference of ΔC^* and ΔC^{DISEQ}, both of which are equally affected by systematic errors in some of the terms, including $R_{C:O}$ [*Chen*, 1993; *Gruber et al.*, 1996; *Gruber*, 1998; *Sabine et al.*, 1999, 2002].

[24] The main difference between the present method and that used by *Gruber et al.* [1996] lies in the expression used

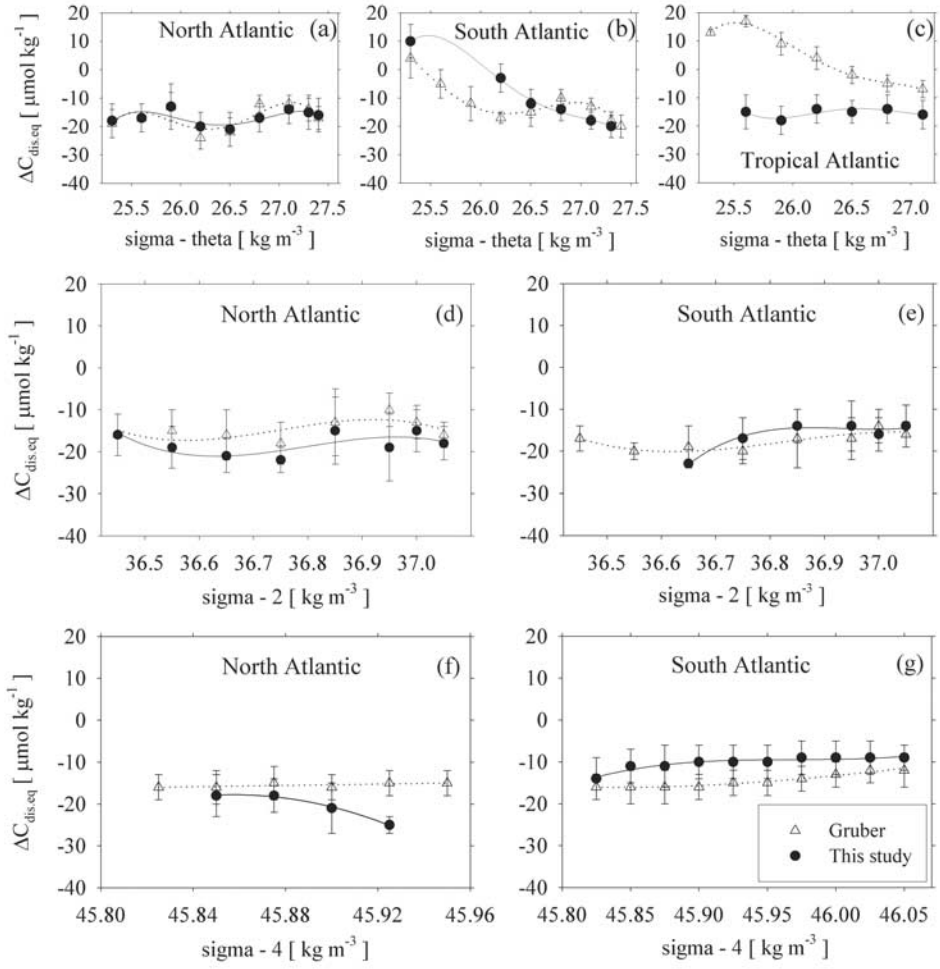

Figure 6. Comparison of estimated air-sea disequilibrium (ΔC^{DISEQ}) (solid circles) with those obtained by *Gruber* [1998] (open triangles). Two independently estimated ΔC^{DISEQ} values are plotted as a function of potential density for the (a, d, f) North Atlantic, (b, e, g) South Atlantic, and (c)Tropical Atlantic. Good agreement is observed except for the tropical Atlantic.

to determine the net air-sea CO_2 disequilibrium value ($\Delta C^{DISEQ\text{-}NET}$) for each sample. Therefore the estimation of the error in the value of C^{ANT} calculated here should include possible errors associated with defining the end-member water types and estimating mixing coefficients using the OMP analysis. The effect on C^{ANT} estimation of errors in end-member water types and mixing coefficients is evaluated in section 4.3, where we estimate the uncertainties in the basin-wide inventory of anthropogenic CO_2.

4. Results and Discussion

4.1. Air-Sea Disequilibrium (ΔC^{DISEQ})

[25] The mean air-sea disequilibrium value (ΔC^{DISEQ}) representing each isopycnal interval is summarized in Table 4 and shown in Figure 6. ΔC^{DISEQ} varies significantly as a function of σ_θ in the main thermocline ($\sigma_\theta = 25.3-27.4$), but changes to lesser extent in the deeper part of the thermocline ($\sigma_2 = 36.45-37.05$) and in deep waters ($\sigma_4 = 45.825-46.050$). All density surfaces denser than $\sigma_\theta > 26.0$ display almost constant but negative values of ΔC^{DISEQ}, suggesting that temperate to high-latitude oceans in which these surfaces outcrop are undersaturated with respect to atmospheric fCO_2. Wintertime cooling in these regions causes the surface fCO_2 to drop below the atmospheric fCO_2 level. The North Atlantic waters have relatively constant ΔC^{DISEQ} values, ranging from -13 to -25 μmol kg^{-1} over the entire water column. In the shallow South Atlantic waters ($\sigma_\theta < 27.2$), the ΔC^{DISEQ} values vary significantly from +10 μmol kg^{-1} in the shallowest density surface to -18 μmol kg^{-1} in the other density surfaces of the tropics.

[26] The ΔC^{DISEQ} values of *Gruber* [1998] estimated from TTO/NAS, TTO/TAS, and SAVE data are also included in Figure 6 for comparison. Gruber used limited $^3H-^3He$ data in the North Atlantic (north of 15°N) and CFC-11 data in the tropical and South Atlantic to estimate the water mass age. Figure 6 shows the spline curves that were used to estimate C^{ANT} by *Gruber et al.* [1996] and *Gruber* [1998]. The largest discrepancies between these curves and our values are found in the upper tropical Atlantic waters

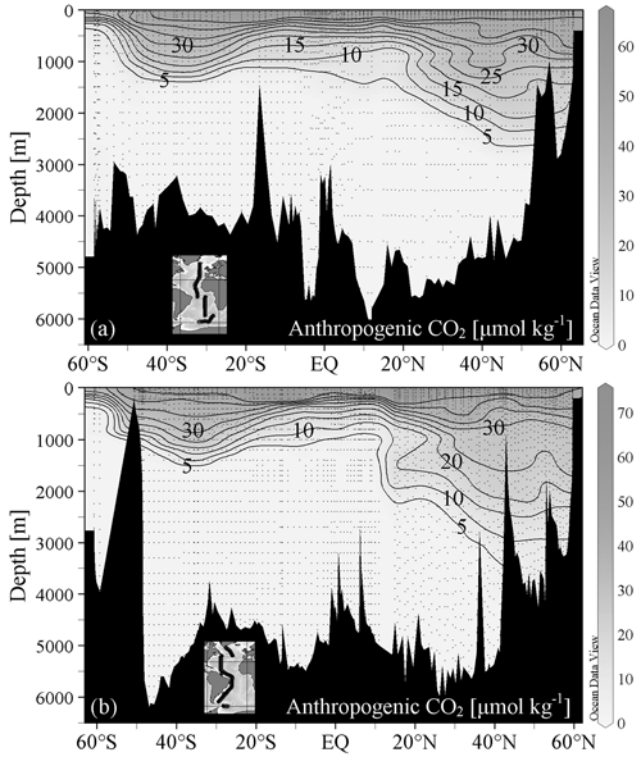

Figure 7. Meridional distributions of anthropogenic CO_2 (μmol kg^{-1}) from 60°N to 60°S in the (a) eastern and (b) western Atlantic.

between $\sigma_\theta = 25.6$ and $\sigma_\theta = 27.1$, where our values are 10 to 30 μmol kg^{-1} lower (Figure 6c). These discrepancies could potentially arise from differences in independently derived empirical relationships for A_T^o, $C_T^{EQ}{}_T$, C_T^{EQ}, or differences between the data sets of present study and those used previously. The empirical relationship for A_T^o applies to the entire water column whereas that for C_T^{EQ} applies only to deep waters uncontaminated by anthropogenic CO_2. If systematic differences exist in these relationships derived from two different data sets, the comparison of the estimated ΔC^{DISEQ} with that of *Gruber* [1998] for the entire water column will reflect these differences. The good agreement between our work and that of *Gruber* [1998] for much of the Atlantic Ocean suggests that this effect is small (Figures 6d–6g). The same contention can also apply to the possible effect of differences between the different data sets. Another possible explanation is that differences in $C_T^{EQ}{}_T$ could be responsible. Differences in age estimation may exist because CFC-12 age was used for estimation of $C_T^{EQ}{}_T$ in the present work whereas CFC-11 or ^{3}H-^{3}He age was used by *Gruber* [1998].

[27] Overall, the reasonable agreement between our work and that of *Gruber* [1998] for much of the Atlantic Ocean indicates good agreement in the values of A_T^o, C_T^{EQ}, and ΔC^{DISEQ}, which were derived independently from two different data sets (TTO/SAVE versus WOCE/JGOFS/OACES). However, it must be remembered that in the present work we used an updated version of Gruber's original ΔC^* calculation method. Hence caution should be exercised when making a direct comparison between the present results and those of *Gruber* [1998].

4.2. Distribution of Anthropogenic CO_2

[28] Figures 7a and 7b show the meridional distributions of anthropogenic CO_2 in the eastern and western Atlantic. The surface concentrations of anthropogenic CO_2 (typically 50–60 μmol kg^{-1}) are highest in the subtropical surface waters and decrease with moving toward high latitudes (30–40 μmol kg^{-1}). This is consistent with the two known phenomena, namely that the accumulation of anthropogenic CO_2 in surface waters depends on the vertical mixing of subsurface waters and that the buffer capacity of seawater with respect to CO_2 addition is temperature dependent. In the subtropical regions, vertical mixing of surface waters with subsurface waters is limited due to strong stratification, which leads to higher values of C^{ANT} in surface waters. At high latitudes, however, surface waters mix with old waters to a greater extent, lowering the value of C^{ANT} in the surface waters. Moreover, differences in the Revelle factor [*Revelle and Suess*, 1957] between low- and high-latitude waters also contribute to the observed differences. Warm waters can absorb considerably more CO_2 than cold water for a given CO_2 increase in the atmosphere.

[29] Anthropogenic CO_2 generally penetrates to shallower depths in the tropical oceans but to deeper depths in the subtropical ocean (30°–40°). The symmetry of vertical penetration of anthropogenic CO_2 about the equator breaks down toward the poles (latitudes >50°). In the northern high-latitude regions, the penetration of anthropogenic CO_2, as defined by a 5 μmol kg^{-1} contour, is greater than 3000 m. The deeper penetration of anthropogenic CO_2 in the northern high-latitude ocean is caused by the sinking and subsequent southward spreading of newly formed North Atlantic Deep water (NADW), which contains significant quantities of anthropogenic CO_2 and other transient tracers such as CFC and bomb ^{14}C [*Doney and Jenkins*, 1994; *Fine*, 1995]. In the South Atlantic (south of 50°S), on the contrary, the value of C^{ANT} falls sharply to below 5 μmol kg^{-1} at a depth of only 500 m, although deep-water formation occurs in the Weddell Sea. *Poisson and Chen* [1987] and *Hoppema et al.* [2001] suggested three probable factors contributing to the shallower penetration and low inventories of anthropogenic CO_2: (1) inhibition of air-sea CO_2 exchange by the extension of sea ice during the winter, (2) significant dilution by mixing with intermediate and deep waters that contain little anthropogenic CO_2, and (3) the short residence time available for newly formed deep waters in this region to pick up anthropogenic CO_2 from the atmosphere. *Caldeira and Duffy* [2000] also suggested that anthropogenic CO_2 absorbed into this region is quickly transported to other regions along shallow isopycnal surfaces. The shallower penetration of anthropogenic CO_2 in the South Atlantic is consistent with measurements of CFCs in the Southern Ocean including Weddell Sea [*Warner and Weiss*, 1992; *Schlosser et al.*, 1994].

[30] The other major feature found in the meridional sections is the effect of the Deep Western Boundary Current (DWBC) on the zonal distribution of anthropogenic CO_2 in

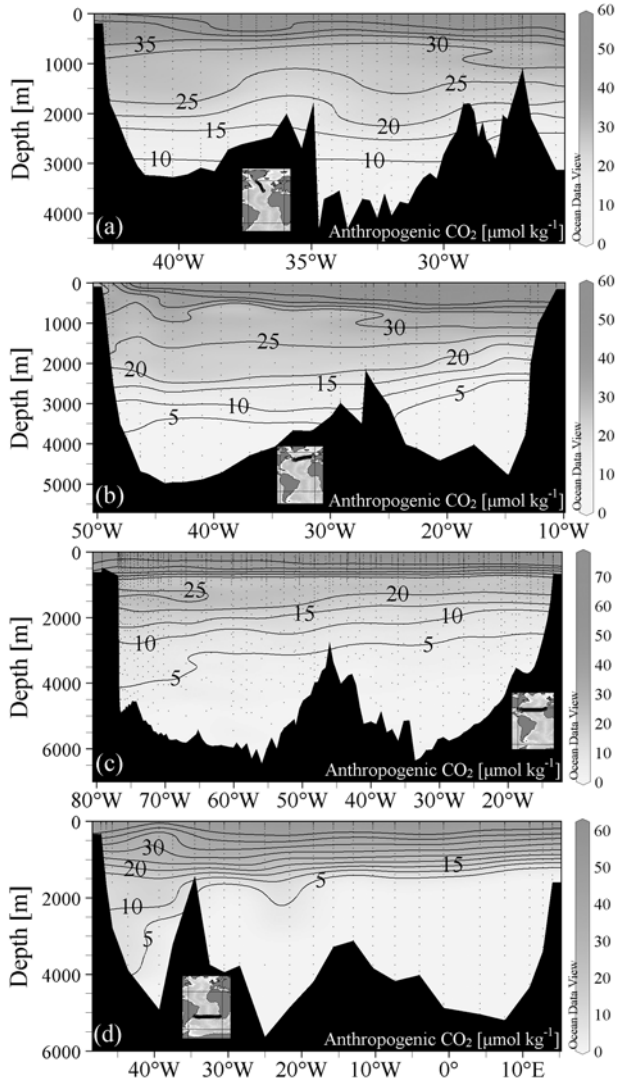

Figure 8. Zonal distributions of anthropogenic CO_2 (μmol kg^{-1}) from 60°W to 20°E nominally along (a) 50°N, (b) 45°N, (c) 27°N, and (d) 30°S.

the North Atlantic. The distribution of CFCs show that the DWBC transports newly formed deep water in the northern high latitudes to the tropics within decades [*Doney and Jenkins*, 1994; *Molinari et al.*, 1998]. Consequently, elevated values of C^{ANT} are expected in the western basin compared to the eastern basin. The vertical penetration and southward spreading of anthropogenic CO_2 in the western basin is much larger than in the eastern basin [*Körtzinger et al.*, 1999], as shown in four zonal sections of C^{ANT} depicted in Figure 8. An interesting feature found in the subtropical western Atlantic is a distinct layer of higher values of C^{ANT} between 1200 m and 1500 m (see Figure 8c). This water mass, known as the Upper Labrador Seawater (LSW), appears to be formed in the Southern Labrador Sea [*Pickart et al.*, 1997] and is characterized by high CFC concentrations and salinity. The higher values of C^{ANT} in this layer compared to the same depth range in the eastern basin is probably due to the southward movement of recently formed LSW charged with high concentrations of anthropogenic CO_2.

[31] The spatial pattern of C^{ANT} in the Atlantic Ocean can also be examined on particular density surfaces. Figures 9a and 9b show the distributions of C^{ANT} on the $\sigma_\theta = 27.10$ and $\sigma_2 = 37.00$ surfaces. These isopycnal surfaces are selected because they represent the Subpolar/Subantarctic Mode Water and the core of the NADW, respectively. On the $\sigma_\theta = 27.10$ isopycnal surface, high values of C^{ANT} extend from the northeast to the southwest, primarily due to anticyclonic gyre transport. On the $\sigma_2 = 37.00$ surface, in contrast, high C^{ANT} values are found in the northwestern part of the North Atlantic and extend southward along the western edge of the North Atlantic. This distribution pattern reflects the pathway of the NADW.

4.3. Inventories of Anthropogenic CO_2

[32] The inventory of anthropogenic CO_2 for each 10° latitude band between 70°S and 70°N, denoted TOTAL-C^{ANT}, was determined by separately integrating the area-weighed mean profile of C^{ANT} (f-C^{ANT}) in the eastern and western basin from the surface (SFC) to a mean bottom depth (MAX) (Table 5),

$$\text{TOTAL} - C^{ANT}(\text{lat.1}, \text{lat.2}) = \int_{SFC}^{MAX} A(\text{lat.1}, \text{lat.2}) f\text{-}C^{ANT} dz, \quad (11)$$

where A (lat. 1, lat. 2) is the area of each latitude band between lat. 1 and lat. 2. The boundaries between the eastern and western basins for each latitude band are nominally set at the location of mid-oceanic ridge. This method was also used to estimate the total inventory of anthropogenic CO_2 absorbed into the Atlantic Ocean using TTO/NAS, TTO/TAS, and SAVE data [*Gruber*, 1998]. Estimated inventories for all latitude bands were summed to produce the basin-wide anthropogenic CO_2 inventory [*Gruber et al.*, 1996; *Gruber*, 1998]. The total amounts of anthropogenic CO_2 that have accumulated in the North Atlantic (equator-70°N) and the South Atlantic (equator-70°S) were found to be 28.4 Pg C and 18.5 Pg C, respectively. These estimated total inventories are assumed to reflect the conditions in 1994, the middle year of the WOCE/JGOFS/OACES Atlantic carbon survey.

[33] We also estimated the potential errors of anthropogenic CO_2 inventories for the North Atlantic and the South Atlantic based on the errors associated with estimating mixing coefficients from the OMP analysis and with defining the end-member water types (see Table 2). Estimated mixing coefficients are subject to errors due to uncertainties in the six measured parameters used in the OMP analysis. Therefore an approximate upper estimate of $\Delta C^{DISEQ\text{-}NET}$ for each data point was calculated by increasing the mean values of all parameters by the standard deviation of the mean value for each water type and then running the OMP routine using these revised values. The resulting mixing fractions were then multiplied by the mean ΔC^{DISEQ} values for all water types contributing to each data point. To obtain a lower estimate of $\Delta C^{DISEQ\text{-}NET}$ for the

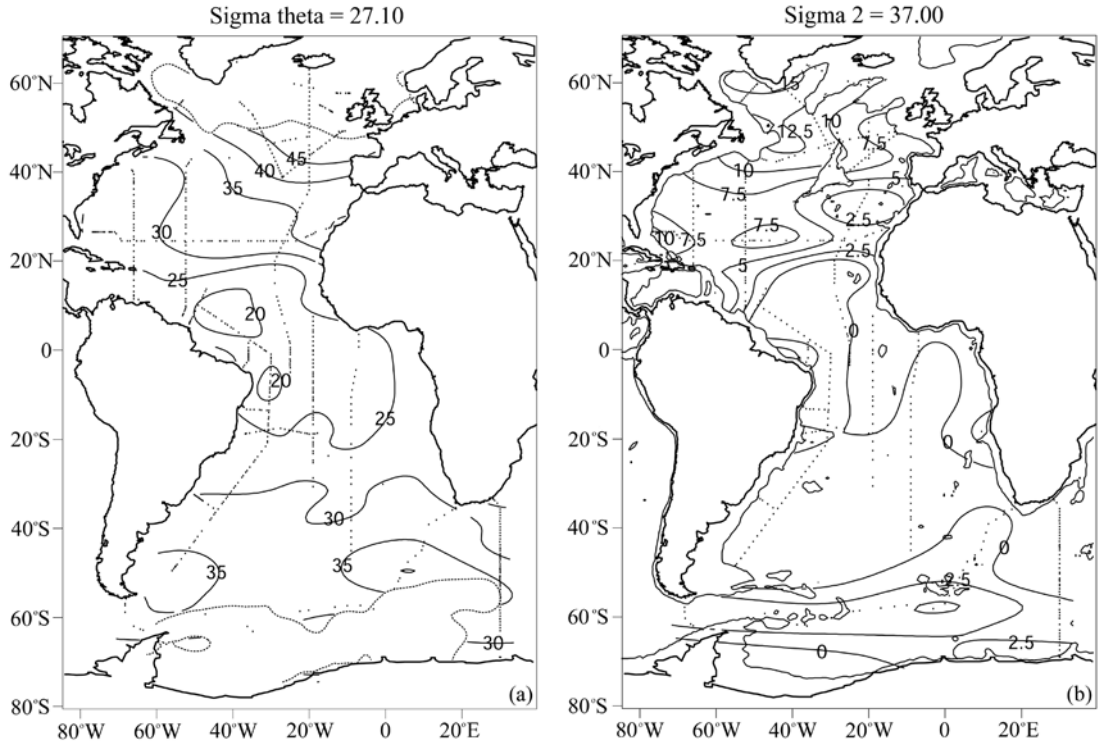

Figure 9. Distribution of anthropogenic CO_2 (μmol kg^{-1}) on the (a) σ_θ = 27.10 and (b) σ_2 = 37.00 surfaces in the Atlantic. These isopycnal surfaces run through the core of the Subpolar/Subantarctic Mode Water and of the North Atlantic Deep water.

same data point, the mean values of all parameters decreased by the standard deviation of the mean and these values were used as inputs for the OMP routine. This analysis yielded an upper and lower limit of the area-weighed mean profile of C^{ANT} for each latitude band. Integration of the revised profiles to their maximum penetration depths yielded an error <1% of the total anthropogenic CO_2 inventory for each latitude band. Using a similar approach, the uncertainties in C^{ANT} caused by errors in the end-member disequilibrium values were estimated by adjusting the mean ΔC^{DISEQ} values by the standard deviation of the mean value for each water type (see Table 2). The resulting adjusted ΔC^{DISEQ} values were then multiplied by the mixing fractions to estimate the approximate upper and lower values of $\Delta C^{DISEQ\text{-}NET}$ for each data point. This analysis yielded an error of about 17% of the total anthropogenic CO_2 inventory for each latitude band, which is significantly greater than that caused by uncertainties in the mixing coefficients but comparable to previous error estimates using the same method [*Gruber et al.*, 1996; *Gruber*, 1998; *Sabine et al.*, 1999, 2002]. The overall uncertainties of the total anthropogenic CO_2 inventory for the North Atlantic and the South Atlantic are about 4.7 Pg C and 3.9 Pg C, respectively.

[34] The highest inventories of TOTAL-C^{ANT} are generally observed in subtropical regions, specifically, between 30°S and 40°S and between 20°N and 30°N (Figure 10a). The maximum in the North Atlantic bands is about 2 Pg C higher than that in the South Atlantic bands. The high-latitude regions have considerably lower total inventories despite the fact that anthropogenic CO_2 has penetrated to the bottom in these regions. This pattern is directly attributable to the lower total volumes of water in high-latitude regions in comparison to the tropics and subtropics. The deeper penetration (3000 m to the bottom) of anthropogenic CO_2 in the high-latitude regions of the North Atlantic is in sharp contrast to the distribution in the North Pacific, where anthropogenic CO_2 has only penetrated to depths shallower than 1500 m, primarily due to a lack of deep-water formation in the North Pacific. Overall, the TOTAL-C^{ANT} inventories for different latitude bands vary considerably; these variations are largely due to differences in the total water volume at different latitudes (Figure 10a).

[35] The distribution of anthropogenic CO_2 accumulation is therefore better represented by the specific column inventories for each latitude block, SPEC-C^{ANT} (mol C m^{-2}), which is calculated by dividing TOTAL-C^{ANT} by the area of each latitude band (A(lat. 1, lat. 2)) (Table 5),

$$\text{SPEC-C}^{\text{ANT}}(\text{lat. 1, lat. 2}) = \text{TOTAL-C}^{\text{ANT}}(\text{lat. 1, lat. 2})/A(\text{lat. 1, lat. 2}). \quad (12)$$

The distribution of the SPEC-C^{ANT} inventory is similar to that of the TOTAL-C^{ANT} inventory in most regions except the North Atlantic, where anthropogenic CO_2 penetrates into deep basins (Figure 10b). The highest specific column inventory is observed between 30°S and 40°S with 53 mol C m^{-2} and between 40°N and 50°N with 78 mol C m^{-2}.

Table 5. Inventory of Anthropogenic CO_2 for Each 10° Latitude Band Between 70°S and 70°N in the Atlantic Ocean

Latitude Belt, deg	West Surface Area, 10^{12} m^2	West Volume, 10^{16} m^3	West Inventory, Pg C	West Specific Inventory, mol C m^{-2}	East Surface Area, 10^{12} m^2	East Volume, 10^{16} m^3	East Inventory, Pg C	East Specific Inventory, mol C m^{-2}	Total Inventory, Pg C	Total Specific Inventory, mol C m^{-2}
70°S–60°S	4.0	1.4	0.3	7.0	0.6	0.3	[a]0.0	5.9	0.3 ± 0.1	7
60°S–50°S	4.6	1.6	1.0	17.8	1.6	0.6	0.3	13.6	1.3 ± 0.2	17
50°S–40°S	4.6	1.9	2.3	41.1	2.9	1.2	1.4	41.5	3.7 ± 0.8	41
40°S–30°S	3.9	1.5	2.6	55.2	3.5	1.4	2.2	51.2	4.8 ± 0.9	53
30°S–20°S	3.6	1.4	2.1	49.8	3.1	1.3	1.6	43.1	3.7 ± 0.6	47
20°S–10°S	3.0	1.4	1.4	39.7	3.1	1.3	1.1	30.6	2.5 ± 0.7	35
10°S–Equator	2.6	1.2	1.0	32.2	3.5	1.4	1.2	29.3	2.2 ± 0.6	31
Total South Atlantic									**18.5 ± 3.9**	
Equator - 10°N	2.6	0.8	0.8	26.7	4.2	1.6	1.6	31.4	2.5 ± 0.8	30
10°N–20°N	4.6	1.6	1.7	31.3	3.4	1.5	1.1	27.8	2.8 ± 1.0	30
20°N–30°N	5.5	2.1	4.2	63.2	3.4	1.5	2.6	62.8	6.8 ± 1.2	63
30°N–40°N	4.2	1.9	3.7	72.8	2.8	1	2.2	66.2	5.9 ± 0.9	70
40°N–50°N	3.2	0.9	2.8	73.6	2.1	0.7	2.1	85.2	4.9 ± 0.4	78
50°N–60°N	2.6	0.5	1.8	58.3	2.2	0.4	1.8	67.7	3.6 ± 0.3	63
60°N–70°N	2.1	0.2	1.0	39.7	1.6	0.2	0.9	45.5	1.9 ± 0.1	42
Total North Atlantic									**28.4 ± 4.7**	

[a]actual value 0.04.

The distribution of the SPEC-C^{ANT} inventory is consistent with that predicted from patterns resulting from thermohaline circulation [*Sarmiento et al.*, 1992]. Moreover, Ekman divergence near the equator and lateral transport of anthropogenic CO_2 from the temperate oceans to the subtropical oceans result in accumulation of anthropogenic CO_2 in the subtropical oceans, which in turn leads to high specific column inventories. The basin-wide distribution of the anthropogenic CO_2 column inventory is more clearly seen in the distribution of anthropogenic CO_2 values (Figure 11) that have been gridded using the objective mapping technique of *LeTraon* [1990].

4.4. Comparison With Gruber's Estimates

[36] *Gruber et al.* [1996] and *Gruber* [1998] applied the ΔC* approach to inorganic carbon data collected from the TTO/NAS, TTO/TAS, SAVE, and two *Meteor* (*Meteor* 11/5 and *Meteor* 15/3) surveys, and estimated basin-wide distribution and inventory of anthropogenic CO_2 in the Atlantic Ocean for the 1980s. The *Meteor* cruises were used in our analysis as well. The surveys in the North Atlantic (TTO/NAS and TTO/TAS) were conducted between 1981 and 1983, while the South Atlantic was sampled between 1987 and 1991 (SAVE, *Meteor* 11/5, and *Meteor* 15/3). The estimated inventories determined by *Gruber* [1998], 21.1 ± 5.0 Pg C for the North Atlantic (equator to 70°N) and 18.0 ± 4.0 Pg C for the South Atlantic (equator to 70°S), were referenced to 1982 and to 1989, respectively.

[37] The total inventory of 28.4 Pg C (referenced to 1994) for the North Atlantic reported here is significantly higher than *Gruber*'s [1998] value of 21.1 Pg C (referenced to 1982) for the same basin. In contrast, our total estimate of 18.5 Pg C (referenced to 1994) for the South Atlantic is similar to the value of 18.0 Pg C (referenced to 1989) obtained by Gruber. For direct comparison of our estimates with Gruber's inventories, the amount of anthropogenic CO_2 taken up by the Atlantic Ocean during the period between TTO(1982)/SAVE(1989) and WOCE/JGOFS/OACES(1994) era was estimated by the Princeton ocean

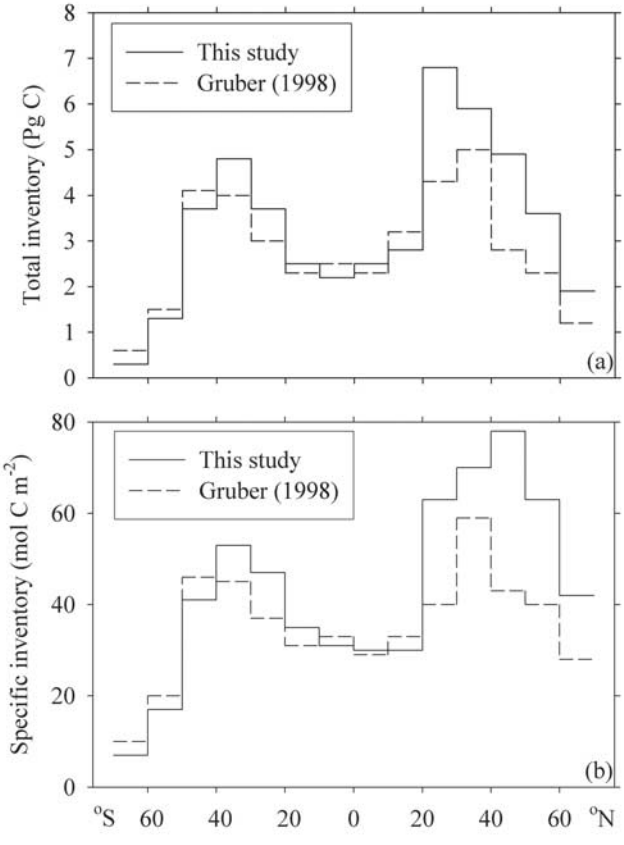

Figure 10. (a) Total and (b) specific inventories of anthropogenic CO_2 between 70°N and 70°S in the Atlantic Ocean. For direct comparison of our estimates with *Gruber*'s [1998] inventories, Gruber's original inventories were scaled up to 25 Pg C for the North Atlantic and 19 Pg C for the South Atlantic by adding the model-predicted increase for the North Atlantic between 1982 and 1994 and for the South Atlantic between 1989 and 1994.

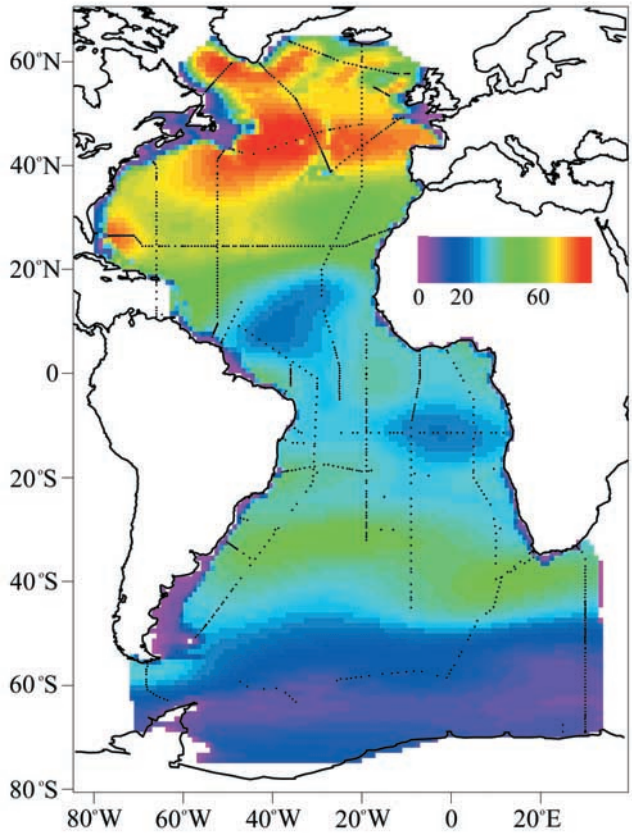

Figure 11. Map of anthropogenic CO_2 column inventory (mol C m^{-2}) in the Atlantic. Circles denote locations of stations.

biogeochemical model (POBM) [*Sarmiento et al.*, 1995]. This model-predicted uptake rate was then used to correct the older estimates to 1994. The POBM predicts an annual uptake rate of 0.25 Pg C yr^{-1} for the North Atlantic and of 0.23 Pg C yr^{-1} for the South Atlantic [*Sarmiento et al.*, 1995; *Gruber*, 1998]. By adding the model-predicted increase of 3 Pg C for the North Atlantic over the period 1982–1994 and of 1.2 Pg C for the South Atlantic over the period 1989–1994, Gruber's estimates scaled up to 25 Pg C for the North Atlantic and 19 Pg C for the South Atlantic. These revised estimates agree with our inventories.

4.5. Anthropogenic CO_2 in the World Oceans

[38] The patterns of the deep-water circulation affect the overall distribution of anthropogenic CO_2 in the oceans. The meridional distribution of anthropogenic CO_2 is mostly symmetric about the equator, with the exception of the North Atlantic, where the formation of DWBC carries anthropogenic CO_2 into the ocean interior. The highest column inventories are observed in the midlatitudes of both hemispheres in all three major basins because of lateral transport of anthropogenic CO_2 into these regions. The third main feature is the small amount of anthropogenic CO_2 in the Southern Ocean (south of 50°S), which was first observed by *Poisson and Chen* [1987] and later confirmed by *Hoppema et al.* [2001].

[39] Inventories of anthropogenic CO_2 estimated independently for three ocean basins in the present work and previous studies [*Sabine et al.*, 1999, 2002] show that the global oceans excluding marginal seas and the Arctic Ocean have absorbed the total of 112 Pg C of anthropogenic CO_2 since the beginning of the Industrial Revolution. This anthropogenic CO_2 is distributed unevenly across the three major basins, with levels of 46.9 ± 8.6 Pg C in 1994 for the Atlantic Ocean, 44.5 ± 5 Pg C in 1994 for the Pacific Ocean, and 20.3 ± 3 Pg C in 1995 for the Indian Ocean. The total inventory of 112 ± 17 Pg C in the world oceans accounts for approximately 29% of the total 387 Pg C of anthropogenic CO_2 that is estimated to have been emitted over the past 250 years by the burning of fossil fuels and cement production (244 Pg C) [*Marland et al.*, 2002] and by land-use change (143 Pg C) [*Houghton and Hackler*, 2002].

5. Conclusions

[40] To estimate the anthropogenic CO_2 inventory of the Atlantic Ocean, we applied the extended ΔC* method to high-quality inorganic carbon, CFC, and nutrient data collected during the WOCE/JGOFS/OACES survey of the Atlantic Ocean between 1990 and 1998. The anthropogenic CO_2 distribution in the Atlantic Ocean determined in the present analysis displays various features that are consistent with those found in the Indian Ocean and Pacific Ocean, most notably, high column inventories in the midlatitude regions and lower column inventories in the Southern Ocean. However, in contrast to other basins, the Atlantic Ocean was found to have high column inventories at latitudes >40°N, largely due to the effective transport of anthropogenic CO_2 by newly formed deep water transported southward in the Deep Western Boundary Current.

[41] The total inventory of anthropogenic CO_2 in the Atlantic Ocean is approximately 46.9 ± 8.6 Pg C that is slightly higher than that of the Pacific Ocean. A method similar to that used here has previously been applied to data for the Indian Ocean [*Sabine et al.*, 1999] and Pacific Ocean [*Sabine et al.*, 2002] collected during the WOCE/JGOFS/OACES global carbon survey. The estimated distribution and inventory of anthropogenic CO_2 for the Atlantic Ocean presented here, in conjunction with the results of the previous analysis for the Indian Ocean and Pacific Ocean, should provide useful constraints for global ocean models used to estimate the uptake of anthropogenic CO_2 and to assess future changes in the oceanic uptake of anthropogenic CO_2 and in the global carbon cycle.

[42] **Acknowledgments.** This work would not have been possible without the efforts of many scientists, particularly those responsible for the carbon, CFC, and nutrients measurements on the ships during the WOCE/JGOFS global CO_2 survey conducted between 1990 and 1998. We wish to thank all of the U.S. and European scientists who contributed to the Atlantic data set that was compiled for the Global Ocean Data Analysis Project (GLODAP), and Nicolas Gruber for constructive suggestions on the manuscript. This work was partially supported by grant R01-2002-000-00549-0 (2003) from the Basic Research Program of the Korea Science and Engineering Foundation (K. L.), by the Brain Korea 21 Project in 2003 (K. L.), by Office of Oceanic and Atmospheric Research of the National Oceanic and Atmospheric Administration (C. S., F. J. M., R. A. F., R. W.,

J. L. B., and T. H. P.), and by the National Science Foundation (C. S., F. J. M., and R. M. K.).

References

Anderson, L. A., and J. L. Sarmiento, Redfield ratios of remineralization determined by nutrient data analysis, *Global Biogeochem. Cycles*, *8*, 65–80, 1994.

Brewer, P. G., Direct observation of the oceanic CO_2 increase, *Geophys. Res. Lett.*, *5*, 997–1000, 1978.

Broecker, W. S., 'NO,' a conservative water-mass tracer, *Earth Planet. Sci. Lett.*, *23*, 100–107, 1974.

Broecker, W. S., T. Takahashi, and T.-H. Peng, Reconstruction of past atmospheric CO_2 contents from the chemistry of the contemporary ocean, *Rep. DOE/OR-857*, 79 pp., U.S. Dept. of Energy, Washington, D. C., 1985.

Caldeira, K., and P. B. Duffy, The role of the Southern Ocean in uptake and storage of anthropogenic carbon dioxide, *Science*, *287*, 620–622, 2000.

Chen, C.-T. A., The oceanic anthropogenic CO_2 sink, *Chemosphere*, *27*, 1041–1064, 1993.

Chen, C.-T., and F. J. Millero, Gradual increase of oceanic CO_2, *Nature*, *277*, 205–206, 1979.

Clayton, T. D., and R. H. Byrne, Calibration of m-cresol purple on the total hydrogen ion concentration scale and its application to CO_2-system characteristics in seawater, *Deep Sea Res., Part I*, *40*, 2115–2129, 1993.

Dickson, A. G., and C. Goyet (Eds.), Handbook of methods for the analysis of the various parameters of the carbon dioxide system in seawater, vol. 2, *ONRL/CDIAC-74*, Dept. of Energy, Washington, D. C., 1994.

Dickson, A. G., and F. J. Millero, A comparison of the equilibrium constants for the dissociation of carbonic acid in seawater media, *Deep Sea Res., Part I*, *34*, 1733–1743, 1987.

Dickson, A. G., J. D. Afghan, and G. C. Anderson, Seawater reference materials for oceanic CO_2 analysis: A method for the certification of total alkalinity, *Mar. Chem.*, *80*, 185–197, 2003.

Doney, S. C., and J. L. Bullister, A chlorofluorocarbon section in the eastern North Atlantic, *Deep Sea Res., Part I*, *39*, 1857–1883, 1992.

Doney, S. C., and W. J. Jenkins, Ventilation of the Deep Western Boundary Current and abyssal western North Atlantic: Estimates from tritium and 3He distributions, *J. Phys. Oceanogr.*, *24*, 638–659, 1994.

Doney, S. C., W. J. Jenkins, and J. L. Bullister, A comparison of ocean tracer dating techniques on a meridional section in the eastern North Atlantic, *Deep Sea Res., Part I*, *44*, 603–626, 1997.

Dutay, J.-C., et al., Evaluation of ocean model ventilation with CFC-11: Comparison of 13 global ocean models, *Ocean Modell.*, *4*(2), 89–120, 2002.

Enting, I. G., C. M. Trudinger, and R. J. Francey, A synthesis inversion of the concentration and $\delta^{13}C$ of atmospheric CO_2, *Tellus, Ser. B.*, *47*, 35–52, 1995.

Fine, R. A., Tracers, time scales, and the thermohaline circulation: The lower limb in the North Atlantic ocean, *Rev. Geophys.*, *33*, 1353–1365, 1995.

Gruber, N., Anthropogenic CO_2 in the Atlantic Ocean, *Global Biogeochem. Cycles*, *12*, 165–191, 1998.

Gruber, N., and J. L. Sarmiento, Global patterns of marine nitrogen fixation and denitrification, *Global Biogeochem. Cycles*, *11*, 235–266, 1997.

Gruber, N., J. L. Sarmiento, and T. F. Stocker, An improved method for detecting anthropogenic CO_2 in the oceans, *Global Biogeochem. Cycles*, *10*, 809–837, 1996.

Hoppema, M., W. Roether, R. G. J. Bellerby, and H. J. W. de Baar, Direct measurements reveal insignificant storage of anthropogenic CO_2 in the abyssal Weddell Sea, *Geophys. Res. Lett.*, *28*, 1747–1750, 2001.

Houghton, J. T., Y. Ding, D. J. Griggs, M. Noguer, P. J. van der Linden, and D. Xiaosu (Eds.), *Climate Change 2001*: *The Scientific Basis*, Cambridge Univ. Press, New York, 2001.

Houghton, R. A., and J. L. Hackler, Carbon flux to the atmosphere from land-use changes, in *Trends*: *A Compendium of Data on Global Change*, Carbon Dioxide Inf. Anal. Cent., Oak Ridge Natl. Lab., U.S. Dept. of Energy, Oak Ridge, Tenn., 2002.

Johnson, K. M., K. D. Wills, D. B. Butler, W. K. Johnson, and C. S. Wong, Coulometric total carbon dioxide analysis for marine studies: Maximizing the performance of an automated gas-extraction system and coluometric detector, *Mar. Chem.*, *44*, 167–188, 1993.

Keeling, C. D., and T. P. Whorf, Atmospheric CO_2 records from sites in the SIO air sampling net work, in *Trends*: *A Compendium of Data on Global Change*, Carbon Dioxide Inf. Anal. Cent., Oak Ridge Natl. Lab., Oak Ridge, Tenn., 2000.

Keeling, R. F., and S. R. Shertz, Seasonal and interannual variations in atmospheric oxygen and implications for the global carbon cycle, *Nature*, *358*, 723–727, 1992.

Körtzinger, A., M. Rhein, and L. Mintrop, Anthropogenic CO_2 and CFCs in the North Atlantic Ocean-A comparison of man-made tracers, *Geophys. Res. Lett.*, *26*, 2065–2068, 1999.

Lee, K., F. J. Millero, R. H. Byrne, R. A. Feely, and R. Wanninkhof, The recommended dissociation constants for carbonic acid in seawater, *Geophys. Res. Lett.*, *27*, 229–232, 2000.

LeTraon, P. Y., A method for optimal analysis of fields with spatially variable mean, *J. Geophys. Res.*, *95*, 13,543–13,547, 1990.

Marland, G., T. A. Boden, and R. J. Andres, Global, regional, and national fossil fuel CO_2 emissions, in *Trends*: *A Compendium of Data on Global Change*, Carbon Dioxide Inf. Anal. Cent., Oak Ridge Natl. Lab., U.S. Dept. of Energy, Oak Ridge, Tenn., 2002.

Merhbach, C., C. H. Culberson, J. E. Hawley, and R. M. Pytkowicz, Measurement of the apparent dissociation constants of carbonic acid in seawater at atmospheric pressure, *Limnol. Oceanogr.*, *18*, 897–907, 1973.

Millero, F. J., Thermodynamics of the carbon dioxide system in the oceans, *Geochim. Cosmochim. Acta*, *59*, 661–677, 1995.

Millero, F. J., J. Z. Zhang, K. Lee, and D. M. Campbell, Titration alkalinity of seawater, *Mar. Chem.*, *44*, 153–156, 1993.

Millero, F. J., D. Pierrot, K. Lee, R. Wanninkhof, R. A. Feely, C. L. Sabine, R. M. Key, and T. Takahashi, Dissociation constants for carbonic acid determined from field measurements, *Deep Sea Res., Part I*, *49*, 1705–1723, 2002.

Molinari, R. L., R. A. Fine, W. D. Wilson, R. G. Curry, J. Abell, and M. S. McCartney, The arrival of recently formed Labrador Sea Water in the Deep Western Boundary Current at 26.5°N, *Geophys. Res. Lett.*, *25*, 2249–2252, 1998.

Neftel, A. E., E. Moor, H. Oeschger, and B. Stauffer, Evidence from polar ice cores for the increase in atmospheric CO_2 in the past two centuries, *Nature*, *315*, 45–47, 1985.

Neill, C., K. M. Johnson, E. Lewis, and D. W. R. Wallace, Accurate headspace analysis of fCO_2 in discrete water samples using batch equilibration, *Limnol. Oceanogr.*, *42*, 1774–1783, 1997.

Orr, J. C., E. Maier-Reimer, U. Mikolajewicz, P. Monfray, J. L. Sarmiento, J. R. Toggweiler, N. K. Taylor, J. Palmer, N. Gruber, C. L. Sabine, C. Le Quéré, R. M. Key, and J. Boutin, Global oceanic uptake of anthropogenic carbon dioxide as predicted by four 3-D ocean models, *Global Biogeochem. Cycles*, *15*, 43–60, 2001.

Pickart, R. S., M. A. Spall, and J. R. N. Lazier, Mid-depth ventilation in the western boundary current system of the sub-polar gyre, *Deep Sea Res., Part I*, *44*, 1025–1054, 1997.

Poisson, A., and C.-T. A. Chen, Why is there little anthropogenic CO_2 in the Antarctic Bottom Water, *Deep Sea Res., Part I*, *34*, 1255–1275, 1987.

Poole, R., and M. Tomczak, Optimum multi-parameter analysis of the water mass structure in the Atlantic Ocean thermocline, *Deep Sea Res., Part I*, *46*, 1895–1921, 1999.

Quay, P. D., B. Tilbrook, and C. S. Wong, Oceanic uptake of fossil fuel CO_2: Carbon-13 evidence, *Science*, *256*, 74–79, 1992.

Revelle, R., and H. E. Suess, Carbon dioxide exchange between atmosphere and ocean and the question of an increase of atmospheric CO_2 during the past decades, *Tellus*, *9*, 18–27, 1957.

Sabine, C. L., R. M. Key, K. M. Johnson, F. J. Millero, A. Poisson, J. L. Sarmiento, D. W. R. Wallace, and C. D. Winn, Anthropogenic CO_2 inventory of the Indian Ocean, *Global Biogeochem. Cycles*, *13*, 179–198, 1999.

Sabine, C. L., R. A. Feely, R. M. Key, J. L. Bullister, F. J. Millero, K. Lee, T.-H. Peng, B. Tilbrook, T. Ono, and C. S. Wong, Distribution of anthropogenic CO_2 in the Pacific Ocean, *Global Biogeochem.*, *16*, 1083, doi:10.1029/2001GB001639, 2002.

Sarmiento, J. L., and N. Gruber, Sinks for anthropogenic carbon, *Phys. Today*, *55*(8), 30–36, 2002.

Sarmiento, J. L., and E. T. Sundquist, Revised budget for oceanic uptake of anthropogenic carbon dioxide, *Nature*, *356*, 589–593, 1992.

Sarmiento, J. L., J. C. Orr, and U. Siegenthaler, A perturbation simulation of CO_2 uptake in an ocean general circulation model, *J. Geophys. Res.*, *97*, 3621–3645, 1992.

Sarmiento, J. L., R. Murnane, and C. LeQuéré, Air-sea transfer and the carbon budget of the North Atlantic, *Philos. Trans. R. Soc. London, Ser. B.*, *348*, 211–219, 1995.

Schlosser, P., B. Kromer, R. Weppernig, H. H. Loosli, R. Bayer, G. Bonani, and M. Suter, The distribution of ^{14}C and ^{39}Ar in the Weddell Sea, *J. Geophys. Res.*, *99*, 10,275–10,287, 1994.

Schmitz, W. J., Jr., *On the World Ocean Circulation*, vol. I, *Some Global Features/North Atlantic Circulation*, *Tech. Rep. WHOI-96-03*, Woods Hole Oceanogr. Inst., Woods Hole, Mass., 1996.

Shiller, A. M., Calculating the oceanic CO_2 increase: A need for caution, *J. Geophys. Res.*, *86*, 11,083–11,088, 1981.

Siegenthaler, U., and J. L. Sarmiento, Atmospheric carbon dioxide and the ocean, *Nature*, *365*, 119–125, 1993.

Sonnerup, R. E., On the relationships among CFC derived water mass ages, *Geophys. Res. Lett.*, *28*, 1739–1742, 2001.

Stocker, T. F., W. S. Broecker, and D. G. Wright, Carbon uptake experiments with a zonally-averaged ocean circulation model, *Tellus, Ser. B*, *46*, 103–122, 1994.

Tomczak, M., A multi-parameter extension of temperature/salinity diagram techniques for the analysis of non-isopycnal mixing, *Prog. Oceanogr.*, *10*, 147–171, 1981.

Walker, S. J., R. F. Weiss, and P. K. Salameh, Reconstructed histories of the annual mean atmospheric mole fractions for the halocarbons CFC-11, CFC-12, CFC-113 and carbon tetrachloride, *J. Geophys. Res.*, *105*, 14,285–14,296, 2000.

Wanninkhof, R., and K. Thoning, Measurement of fugacity of CO_2 in surface water using continuous and discrete sampling methods, *Mar. Chem.*, *44*, 189–204, 1993.

Wanninkhof, R., T.-H. Peng, B. Huss, C. L. Sabine, and K. Lee, Comparison of inorganic carbon system parameters measured in the Atlantic Ocean from 1990 to 1998 and recommended adjustments, *ORNL/CDIAC-140*, 43 pp., Oak Ridge Natl. Lab., U.S. Dept. of Energy, Oak Ridge, Tenn., 2003.

Warner, M. J., and R. F. Weiss, Chlorofluoromethanes in the South Atlantic Antarctic Intermediate Waters, *Deep Sea Res., Part I*, *39*, 2053–2075, 1992.

Warner, M. J., J. L. Bullister, D. P. Wisegarver, R. H. Gammon, and R. F. Weiss, Basin-wide distributions of chlorofluorocarbons CFC-11 and CFC-12 in the North Pacific: 1985–1989, *J. Geophys. Res.*, *101*, 20,525–20,542, 1996.

WOCE Data Products Committee, WOCE global data, version 3, *Rep. 180/02*, WOCE Int. Project Off., Southampton, England, 2002.

You, Y., and M. Tomczak, Thermocline circulation and ventilation in the Indian Ocean derived from water mass analysis, *Deep Sea Res., Part I*, *40*, 13–56, 1993.

J. L. Bullister, R. A. Feely, and C. L. Sabine, Pacific Marine Environmental Laboratory, NOAA, 7600 Sand Point Way NE, Seattle, WA 98115, USA. (bullister@pmel.noaa.gov; feely@pmel.noaa.gov; sabine@pmel.noaa.gov)

S.-D. Choi, K. Lee (corresponding author), and G.-H. Park, School of Environmental Science and Engineering, Pohang University of Science and Technology, San 31, Hyoja-dong, Nam-gu, Pohang, 790-784, Republic of Korea. (skills@postech.ac.kr; ktl@postech.ac.kr; pgh3715@postech.ac.kr)

R. M. Key, Atmospheric and Oceanic Sciences Program, Princeton University, Forrestal Campus/Sayre Hall, Princeton, NJ 08544, USA. (key@princeton.edu)

A. Kozyr, Carbon Dioxide Information Analysis Center, Environmental Sciences Division, Oak Ridge National Laboratory, U.S. Deparment of Energy, Building 1509, Mail Stop 6335, Oak Ridge, TN 37831-6335, USA. (kozyra@ornl.gov)

F. J. Millero, Rosenstiel School of Marine and Atmospheric Studies, University of Miami, 4600 Rickenbacker Causeway, Miami, FL 33149, USA. (fmillero@rsmas.miami.edu)

T.-H. Peng and R. Wanninkhof, Atlantic Oceanographic and Meteorological Laboratory, NOAA, 4301 Rickenbacker Causeway, Miami, FL 33149, USA. (peng@aoml.noaa.gov; rik.wanninkhof@noaa.gov)